

Global Teleconnections in Response to a Shutdown of the Atlantic Meridional Overturning Circulation*

LIXIN WU, CHUN LI, AND CHUNXUE YANG

Physical Oceanography Laboratory, Ocean University of China, Qingdao, China

SHANG-PING XIE

International Pacific Research Center and Department of Meteorology, University of Hawaii at Manoa, Honolulu, Hawaii

(Manuscript received 23 January 2007, in final form 14 November 2007)

ABSTRACT

The global response to a shutdown of the Atlantic meridional overturning circulation (AMOC) is investigated by conducting a water-hosing experiment with a coupled ocean–atmosphere general circulation model. In the model, the addition of freshwater in the subpolar North Atlantic shuts off the AMOC. The intense cooling in the extratropical North Atlantic induces a widespread response over the global ocean. In the tropical Atlantic, a sea surface temperature (SST) dipole forms, with cooling north and warming on and south of the equator. This tropical dipole is most pronounced in June–December, displacing the Atlantic intertropical convergence zone southward. In the tropical Pacific, a SST dipole forms in boreal spring in response to the intensified northeast trades across Central America and triggering the development of an El Niño-like warming that peaks on the equator in boreal fall. In the extratropical North Pacific, a basinwide cooling of $\sim 1^{\circ}\text{C}$ takes place, with a general westward increase in intensity.

A series of sensitivity experiments are carried out to shed light on the ocean–atmospheric processes for these global teleconnections. The results demonstrate the following: ocean dynamical adjustments are responsible for the formation of the tropical Atlantic dipole; air–sea interaction over the tropical Atlantic is key to the tropical Pacific response; extratropical teleconnection from the North Atlantic is most important for the North Pacific cooling, with the influence from the tropics being secondary; and the subtropical North Pacific cooling propagates southwestward from off Baja California to the western and central equatorial Pacific through the wind–evaporation–SST feedback.

1. Introduction

The Atlantic meridional overturning circulation (AMOC) is an important component of global climate system (e.g., Broecker 1991; Weaver et al. 1999). Recent interests in it arise partly from concerns about its potential shutdown and subsequent abrupt climate change in response to the modern global warming (e.g., Broecker 2003; Curry et al. 2003). Climate models have shown that freshwater forcing of the subpolar North

Atlantic can lead to a weakening or a collapse of the AMOC, with far-reaching climatic impacts through both atmospheric and oceanic teleconnections (e.g., Dong and Sutton 2002; Zhang and Delworth 2005; Timmermann et al. 2005). Paleoclimate observations indicate that variability coherent with subpolar North Atlantic climate anomalies is ubiquitous around the globe (Broecker 2003; Hemming 2004; Pahnke et al. 2007). So-called water-hosing experiments with coupled ocean–atmosphere general circulation models (GCMs), in which freshwater is artificially added over the subpolar North Atlantic to slow down AMOC (Manabe and Stouffer 1995), prove useful shedding light on the global response to AMOC changes. Several robust response patterns emerge from recent intercomparison of water-hosing experiments among different GCMs, including the meridional dipole of sea surface temperature (SST) decrease and increase over the tropical North and South Atlantic, respectively (Stouf-

* International Pacific Research Center Publication Number 492 and School of Ocean and Earth Science and Technology Publication Number 7231.

Corresponding author address: Lixin Wu, Physical Oceanography Laboratory, Ocean University of China, 5 Yushan Road, Qingdao 266003, China.
E-mail: lxwu@ouc.edu.cn

fer et al. 2006; Timmermann et al. 2007). The present study investigates the mechanisms for the global response to an AMOC shutdown by conducting a suite of experiments to explore ocean–atmospheric teleconnection pathways.

A prominent response of the Atlantic climate to a weakening of the AMOC is a southward shift of the Atlantic intertropical convergence zone (ITCZ), a change seen in both paleoclimate proxy records and coupled GCMs. Recent sediment core records from the Cariaco Basin suggest that the ITCZ–trade wind complex over the tropical Atlantic is tightly linked to the climate over the high-latitude North Atlantic over a wide range of time scales from decadal to glacial–interglacial (e.g., Black et al. 1999; Peterson et al. 2000). In a coupled GCM, Manabe and Stouffer (1988) found that an “off” state of the AMOC leads to cold conditions in the tropical North Atlantic and a southward migration of the ITCZ. All the water-hosing experiments examined by Stouffer et al. (2006) and Timmermann et al. (2007) display a southward shift of the Atlantic ITCZ (see also Vellinga et al. 2002), a response quickly established 4–6 yr after the water hosing (Dong and Sutton 2002). The mechanism leading to this tropical response, however, remains unclear. In general, there are several possible pathways from the extratropical to tropical Atlantic (Chiang 2004). A frequently invoked mechanism is a reduction of the meridional oceanic heat transport associated with an AMOC shutdown (Yang 1999). Another plausible mechanism is via atmospheric response to extratropical North Atlantic cooling, which intensifies the northeast trade winds and displaces the ITCZ through the wind–evaporation–SST (WES) feedback (Xie and Tanimoto 1998; Marshall et al. 2001; Czaja et al. 2002; Chiang 2004). While ocean adjustments in AMOC heat transport are slow and may take years to decades (Goodman 2001), the tropical response to AMOC changes through atmospheric and coupled processes is much more rapid.

Response to an AMOC shutdown is also reported over the tropical Pacific in several recent modeling studies (Dong and Sutton 2002, 2007; Zhang and Delworth 2005; Timmermann et al. 2005, 2007; Stouffer et al. 2006), although the pattern and amplitude vary from one model to another. The interbasin influence is conjectured to be through either large-scale atmospheric circulation changes due to anomalous diabatic heating in the tropical Atlantic (Dong and Sutton 2002; Zhang and Delworth 2005) or oceanic waves transmitted from the North Atlantic to the tropical Pacific (Cessi et al. 2004; Timmermann et al. 2005). In a related experiment, Wu et al. (2005) explicitly demonstrated that

SST anomalies over the tropical North Atlantic trigger an El Niño–like SST development in the tropical Pacific through the coupled WES feedback and the meridional shift of the eastern Pacific ITCZ. A robust Pacific response to tropical North Atlantic cooling is also reported in a high-resolution regional coupled model that reasonably resolves the Central American isthmus (Xie et al. 2007). Timmermann et al. (2007) showed that the variance of El Niño–Southern Oscillation (ENSO) increases in response to water hosing in five GCMs examined, and suggested that the decreased amplitude of the equatorial annual cycle is responsible via nonlinear frequency entrainment mechanisms. Alternatively Dong and Sutton (2007) suggested that changes in linear stability cause the intensified ENSO in the Third Hadley Centre Coupled Ocean–Atmosphere General Circulation Model (HadCM3). Thus, the tropical Pacific response to Atlantic cooling, both in the mean state and annual cycle, display quite some differences in spatial pattern and sign. Further studies are necessary to sort out these differences.

Timmermann et al. (2007) identified the extratropical North Pacific cooling as another robust feature common to all the GCMs in response to the North Atlantic water hosing. This extratropical North Pacific response is due presumably to atmospheric teleconnection through either the advection of the North Atlantic cooling by the mean westerlies and/or the changes of Northern Hemisphere atmospheric circulation. Given its large magnitude, the intensive cooling over the mid-latitude North Pacific can possibly affect the tropical Pacific through atmospheric and oceanic teleconnections (see a recent review by Liu and Alexander 2006). Generally, extratropical-to-tropical teleconnection may involve the shallow meridional overturning circulation (e.g., McCreary and Lu 1994), atmospheric teleconnection (e.g., Barnett et al. 1999; Vimont et al. 2003), and the coupled WES process (Wu et al. 2007b). It remains unclear whether and how the AMOC changes trigger such an extratropical to tropical teleconnection over the Pacific.

This study examines global teleconnections in response to a shutdown of the AMOC, from the subpolar to tropical Atlantic, and across the basin boundaries from the Atlantic to the Pacific. We conduct a series of GCM experiments based on a “modeling surgery” strategy developed in Wu et al. (2003) to explicitly test the effects of key teleconnective processes, complementary to most of water-hosing studies that are based on the diagnosis of one single perturbation experiment. We specifically address the following questions: 1) How do the AMOC changes affect the tropical Atlantic

ITCZ? 2) What are the roles of the tropical Atlantic air–sea coupling and 3) Northern Hemispheric atmospheric teleconnection in transmitting the AMOC influence to the tropical Pacific? The modeling surgery is effective in addressing these questions. For example, the question 2 may be addressed by shutting off ocean–atmospheric coupling in the tropical Atlantic in our coupled GCM.

The rest of the paper is constructed as follows. Section 2 briefly describes the coupled model and changes in the AMOC in the water-hosing experiment. Section 3 discusses the AMOC influence on Atlantic climate, in both the tropics and extratropics. Section 4 studies the Pacific response. Section 5 is a summary with further discussions.

2. Coupled model and experiment design

We use the Fast Ocean–Atmosphere Model (FOAM), version 1.5, a fully coupled global model developed at University of Wisconsin. This is the improved version of the original FOAM (version 1.0), which is described in detail in Jacob (1997). The atmospheric model is a parallel version of the National Center for Atmospheric Research (NCAR) Community Climate Model, version 2 (CCM2), but the atmospheric physics is replaced with those of CCM3. The ocean model was developed following the Geophysical Fluid Dynamics Laboratory (GFDL) Modular Ocean Model (MOM). The FOAM used here has an atmospheric resolution of R15 with 18 vertical levels, and an oceanic resolution of 1.4° latitude \times 2.8° longitude with 32 vertical levels. The coupled model has a thermodynamic sea ice component. Without flux adjustment, the fully coupled control simulation has been integrated for over 1000 yr, without apparent climate shift. FOAM captures major features of the observed climatology (Jacob 1997). FOAM also produces reasonable climate variability, such as ENSO (Liu et al. 2000), tropical Atlantic variability (Wu and Liu 2002), and North Atlantic climate variability (Wu and Liu 2005).

The control simulation with preindustrial greenhouse gases concentration maintains a stable AMOC, but with a somewhat strong intensity (Fig. 1a). The maximum transport is located around 55°N at 35 Sv ($1 \text{ Sv} \equiv 10^6 \text{ m}^3 \text{ s}^{-1}$). However, the outflow of the North Atlantic Deep Water (NADW) is about 18 Sv, which is comparable to most of state-of-the-art GCM simulations (e.g., Stouffer et al. 2006) and current observations (e.g., Talley et al. 2003). The simulated AMOC attains an outflow of the NADW of about 12 Sv at the equator, but the inflow of the Antarctic Bottom Water is very weak. In spite of these deficiencies in simulat-

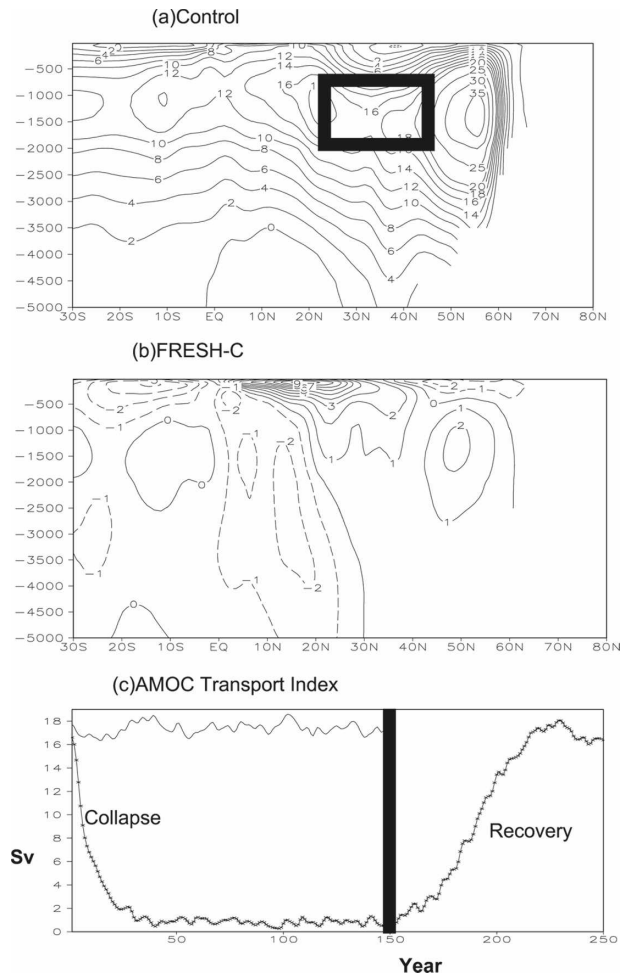


FIG. 1. Mean AMOC in the (a) CTRL and (b) FRESH-C runs. (c) Time series of the AMOC transport index in the CTRL (thin) and FRESH-C runs. In the latter, a 1-Sv freshwater forcing is applied for 0–150 yr. The box in (a) denotes the domain for calculating the transport index.

ing the mean meridional circulation, we believe that the model may be used to assess the global ocean–atmosphere response to a shutdown of the Atlantic AMOC since the local meridional recirculation in the high latitudes has little contribution to the overall ocean meridional heat transport. The present study focuses on the climatic influence of the AMOC, rather than the dynamics of the AOMC itself.

Like most of water-hosing experiments (e.g., Stouffer et al. 2006), a freshwater flux of 1.0 Sv is applied over the North Atlantic from 50° to 70°N , and the model is integrated for 150 yr under this anomalous freshwater forcing. This fully coupled experiment is named FRESH-C, which serves as the reference run for other sensitivity experiments. The AMOC collapses rapidly within the first two decades followed by a slow adjust-

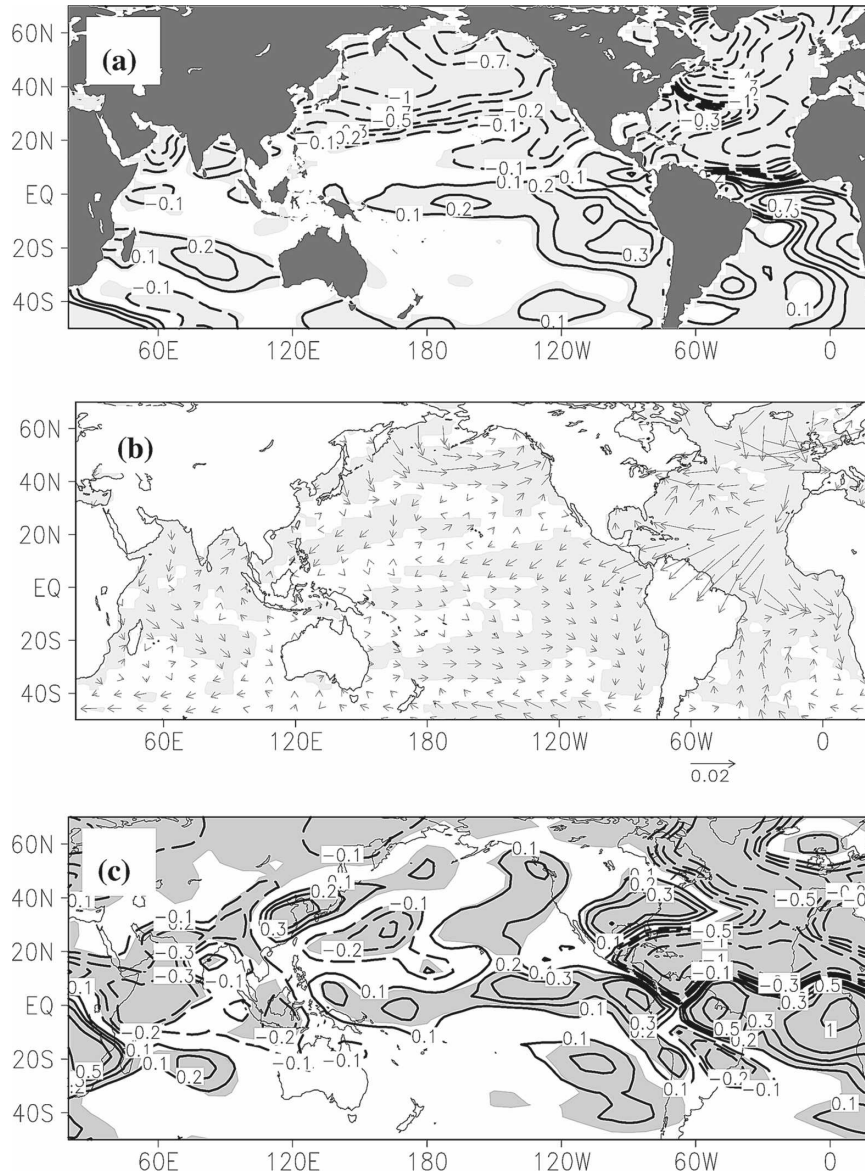


FIG. 2. Annual mean anomalies in FRESH-C: (a) SST ($^{\circ}\text{C}$), (b) surface wind (N m^{-2}), and (c) precipitation (mm day^{-1}). Values over the shaded areas exceed the 95% statistical significance level using a t test.

ment (Fig. 1c). The last 100-yr mean of the meridional overturning circulation demonstrates very weak deep-water formation over the subpolar North Atlantic and a nearly complete collapse of the AMOC (Fig. 1b). After the anomalous freshwater forcing is eliminated at the 150th year, it takes about 70 yr for the AMOC to bounce back to the original strength (Fig. 1c). The recovery time is longer than the collapse time, consistent with other GCM studies (Stouffer et al. 2006). Thus, the model displays a reasonable response of the AMOC, albeit a strong one, to the imposed freshwater forcing over the North Atlantic.

3. Atlantic response

As in most of GCM water-hosing simulations (Stouffer et al. 2006), the annual mean response of Atlantic SST exhibits an interhemispheric seesaw pattern (Fig. 2a), with a maximum cooling of about -7°C over the subpolar North Atlantic, and a second maxima of about -2°C over the tropical North Atlantic, and some modest warming in the South Atlantic with a maximum of 1°C near the equator and the southern African coast. The intense cooling in the high-latitude North Atlantic is partly due to the southward extension

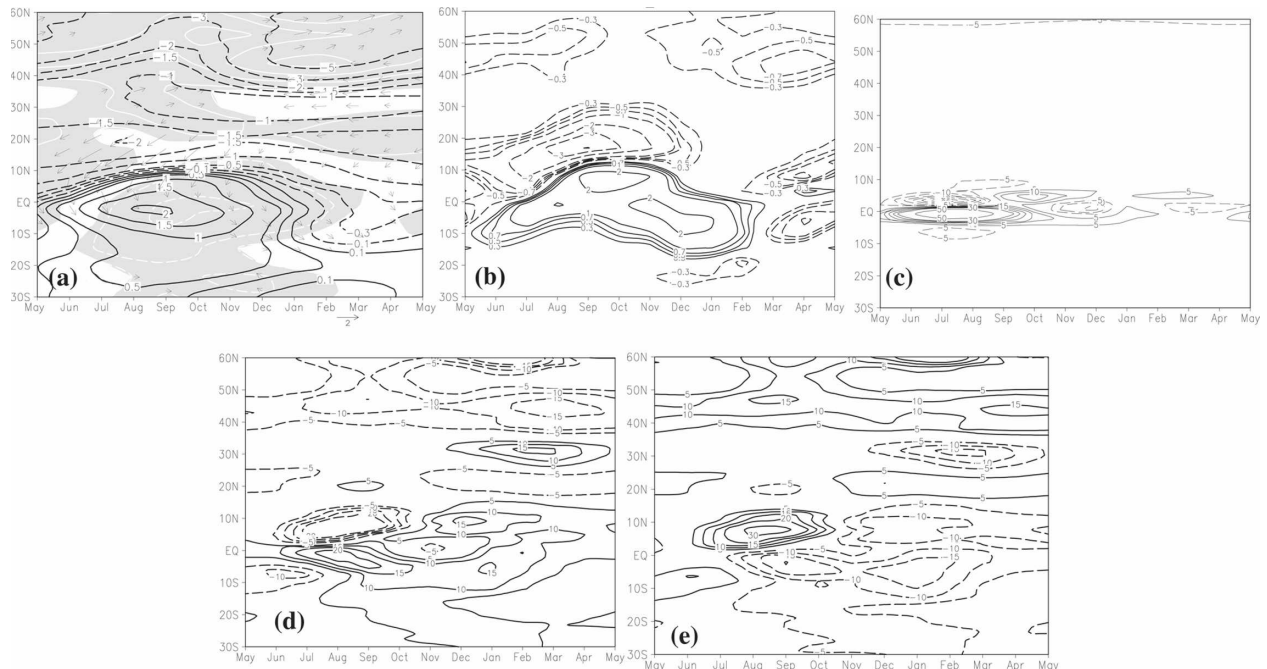


FIG. 3. Time-latitude plots of zonally averaged anomalies across the Atlantic basin: (a) SST (contours), surface wind [vectors; m s^{-1} . The definition of wind direction follows: right (left) arrow = westward (eastward), up (down) arrow = northward (southward); hereafter the arrows have the same meaning], and turbulent heat flux (W m^{-2} ; white contours at 5 W m^{-2} intervals; shade $>3 \text{ W m}^{-2}$; positive-downward); (b) precipitation (mm day^{-1}). Divergence of ocean heat transport (W m^{-2}) of the mixed layer (integrated over the upper 50 m and zonally averaged across the Atlantic basin): (c) vertical, (d) total, and (e) net surface heat flux. Only values exceeding 95% statistical significance are plotted in (a) and (b).

of sea ice during winter and spring. Over the subpolar North Atlantic (50° – 60°N), the SST cooling is associated with an intensification of the westerly winds (Fig. 2b). In the tropics, the anomalous winds display a C-shape pattern: northeasterly north, northerly on, and northwesterly south of the equator. Coupled with this large-scale change of the trade winds is a southward shift of the Atlantic ITCZ (Fig. 2c), with a decrease of precipitation north of the equator ($\sim 1 \text{ mm day}^{-1}$) including the Sahel ($\sim 0.5 \text{ mm day}^{-1}$), and an increase of precipitation of $\sim 0.5 \text{ mm day}^{-1}$ south of the equator including northeast and southern Africa. Such shifts in precipitation pattern, along with the changes in the northeast trades, are considered to give rise to variability observed in the Cariaco Basin sediment core (Peterson et al. 2000) and land-based paleo proxies in South America (Wang et al. 2004; Chiang and Koutavas 2004). Such paleo variability in the tropical Atlantic displays high coherence with the Greenland ice core record, consistent with the water-hosing simulations. On the eastern U.S. seaboard, precipitation increases and the North Atlantic cooling reaches a local minimum offshore, consistent with other GCM simulations (Timmermann et al. 2007).

The ocean-atmospheric response over the Atlantic

exhibits a distinct seasonality (Fig. 3a). Over the subpolar North Atlantic, the anomalous cooling is stronger in cold seasons (winter and spring), twice of that in warm seasons, because of the decelerated deep convection and strengthened westerly winds during winter. Associated with the strong cooling, surface wind anomalies are westerly and easterly in the subpolar (45° – 60°N) and subtropical (20° – 40°N) regions, respectively. The winter anomalous circulation over the North Atlantic displays an equivalent barotropic structure, with a high pressure belt in the midlatitudes to the subtropics and a low pressure cap over the entire Arctic, resembling the positive phase of the Arctic Oscillation–North Atlantic Oscillation (AO–NAO; Figs. 4a,b). The height difference between the high-latitude low and subtropical high is about 10 and 40 gpm at 850 and 250 mb per degree subpolar North Atlantic cooling, respectively, consistent with previous atmospheric GCM studies (e.g., Kushnir et al. 2002). In contrast, the atmospheric response in summer is largely baroclinic (Figs. 4c,d) and extends southward, associated with the tropical North Atlantic cooling (e.g., Wu et al. 2007a). In the fall, the atmospheric response is much reduced at both lower and upper levels (Figs. 4e,f). Although the detailed mechanism for the seasonality of the atmospheric

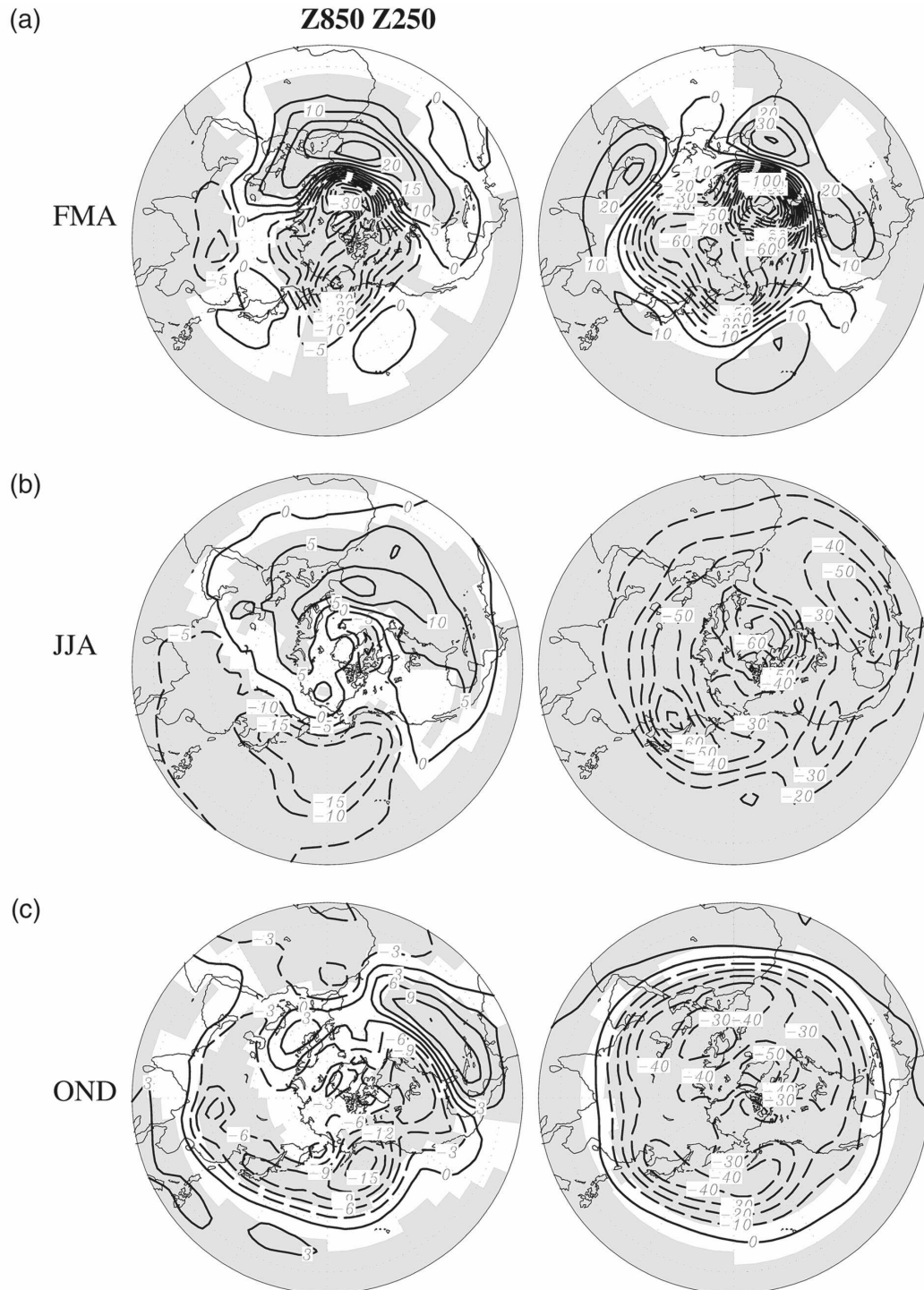


FIG. 4. Geopotential height (gpm) anomalies at (left) 850 and (right) 250 mb in FRESH-C for (a) February–April (FMA), (b) June–August (JJA), and (c) October–December (OND). Values over the shaded areas exceeded the 95% statistical significance level using a t test.

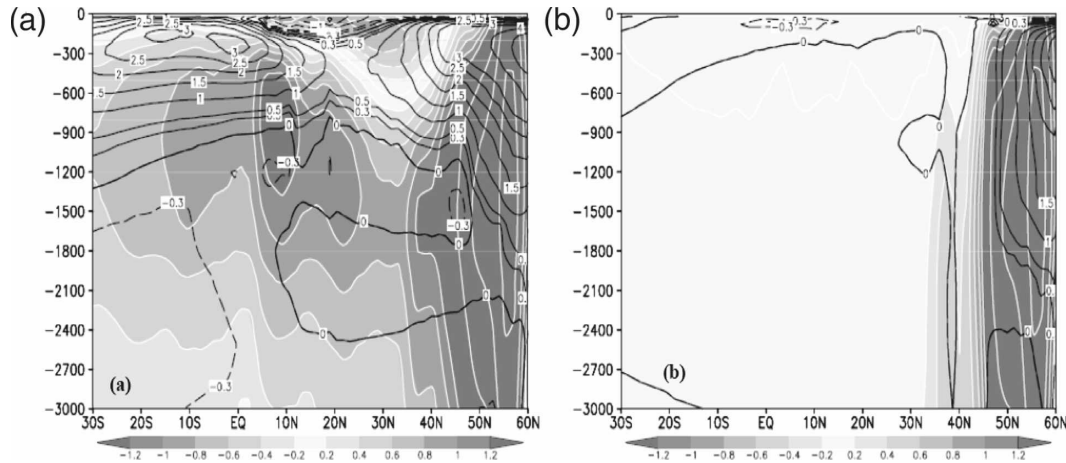


FIG. 5. Latitude–depth sections of overturning heat transport anomalies [shaded with white contours with interval at 0.1 PW (10^{15} W)] zonal mean anomalies of temperature (black contours; $^{\circ}\text{C}$). (a) FRESH-C minus CTRL; (b) PB-NA minus CTRL.

response is beyond the scope of the current study, the equivalent barotropic AO–NAO-like response in winter is likely to involve nonlinear interaction of synoptic eddies, stationary waves, and the jet stream (e.g., Peng et al. 2003) while the baroclinic response in the summer subtropics is likely induced by the deep diabatic cooling associated with the southward shift of the ITCZ (Hoskins and Karoly 1981; Okumura et al. 2001).

In the tropical Atlantic, the cooling north of the equator persists year round, but the cross-equatorial SST gradient and wind anomalies exhibit strong seasonal variations (Fig. 3a). The South Atlantic warming strengthens in boreal summer and fall but is replaced by weak cooling in winter and spring. During much of the year, precipitation decreases north and increases south of the equator (Fig. 3b). This precipitation dipole is most pronounced during June to December when the SST dipole is most fully developed with large South Atlantic warming of up to 2°C . The nodal line of the SST dipole is displaced north of the equator during boreal summer to fall as strong meridional asymmetry develops in the mean state of tropical Atlantic climate (Okajima et al. 2003). The simultaneous development of the SST and precipitation dipoles suggests the interaction between the ocean and atmosphere during June–December. Indeed, the C-shape wind pattern, with the intensified northeast and reduced southeast trades north and south of the equator, respectively, is characteristic of the WES feedback (Xie and Philander 1994). The WES feedback, however, appears to be insufficient to overcome the SST damping due to the Clausius–Claparon equation, with net surface heat flux anomalies acting to damp the SST anomalies.

Ocean dynamics plays an important role in creating

SST anomalies in the tropics. This can be inferred from the latitudinal distribution of zonally averaged net surface heat flux and divergence of oceanic heat transport over the Atlantic basin (Figs. 3d,e). It can be seen that the warming over the south tropical Atlantic is predominantly associated with the convergence of oceanic heat transport (Fig. 3d), with the surface heat flux playing a damping role (Fig. 3e). Near the equator, anomalous northerly cross-equatorial winds drive an anomalous downwelling (upwelling) south (north) of the equator (Fig. 3a). In the control run (CTRL), the southeasterly winds prevail on the equator, especially during May–September, causing upwelling slightly south of the equator. This southern upwelling weakens in FRESH-C in response to the northerly wind anomalies on the equator, causing an anomalous warming on and south of the equator (Fig. 3c). Indeed, the SST warming in FRESH-C peaks slightly south of the equator and during boreal summer and fall when the mean southeasterlies prevail there. Over the north tropical Atlantic, the cooling appears to be associated with the oceanic heat transport divergence in summer, but associated with the surface heat flux over the rest of year (damped by the oceanic heat transport convergence). To further demonstrate the role of thermohaline circulation changes in triggering oceanic warming over the equator and the South Atlantic, the overturning heat transport, defined as $\rho C_p \int_{-H}^z \int_{X_e}^{X_w} \bar{v} T dx dz$ (ρ is density, C_p is heat capacity, \bar{v} is zonally averaged meridional velocity across the Atlantic basin, and X_e and X_w are the eastern and western boundaries of the Atlantic basin) is calculated (Fig. 5). In the FRESH-C, the AMOC shutdown decreases the overturning heat transport, with a peak located around 12°N at the surface

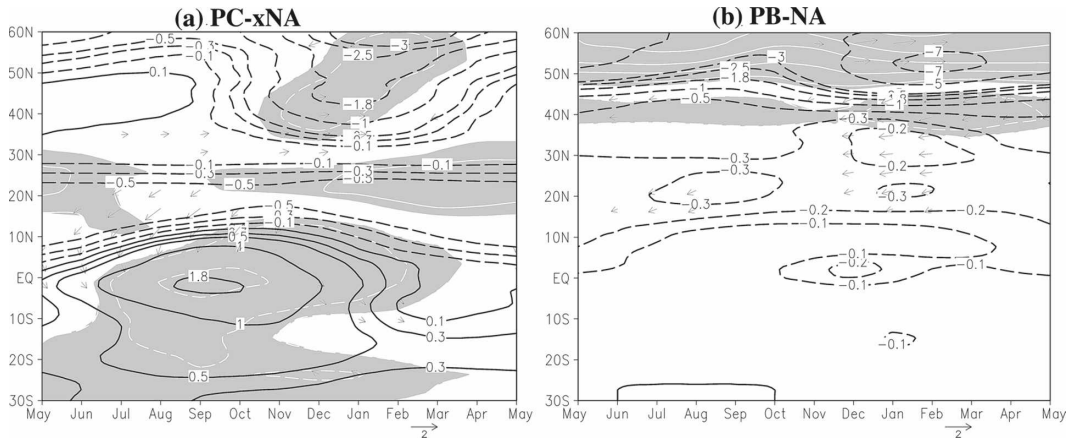


FIG. 6. Same as Fig. 3a, but for (a) PC-xNA in which air–sea coupling is disabled in the extratropical North Atlantic, and (b) PB-NA in which the extratropical–tropical oceanic pathway is deactivated. Values over the shaded areas exceed the 95% statistical significance level using a *t* test.

and shifting poleward with depth. This leads to a heat convergence south of these latitudes, inducing ocean column warming over the entire upper ocean down to about 1000 m, except the surface of the North Atlantic. The shallow cooling over the north tropical and subtropical Atlantic appears to be not directly associated with the heat transport divergence, where the surface heat flux plays an important role (Figs. 3d,e). This result about the importance of ocean circulation changes for tropical SST is broadly consistent with Yang's (1999) ocean GCM results, but the spatial pattern of SST anomalies is very different between two studies, indicative of the importance of ocean–atmosphere interaction.

a. Sensitivity experiments

The above analysis suggests that both oceanic and atmospheric pathways are important for tropical Atlantic anomalies. In this subsection, two additional experiments are carried out by turning off atmospheric and oceanic teleconnections one at a time. In the first experiment, air–sea coupling is disabled over the extratropical North Atlantic (north of 30°N) by using a partial-coupling (PC) modeling strategy (Wu et al. 2003). In this experiment (referred to as PC-xNA), the atmosphere over the PC region is forced by the model climatological SST while the ocean is still forced by the model atmosphere (e.g., the model predicted SST is used for surface heat flux). The ocean and the atmosphere are fully coupled outside of the PC region. Thus, the influence of the extratropical North Atlantic on the tropics through atmospheric teleconnection is eliminated. In the second experiment, we insert a sponge wall in the ocean model between 30° and 40°N from the

surface to the bottom to block the oceanic teleconnection. This partial-blocking (PB; Wu et al. 2003) scheme is implemented by restoring the ocean temperature and salinity to the model climatology. This experiment is referred to as PB-NA. To account for the slight model climate drift caused by the PC or PB scheme, a parallel experiment is performed with the same configuration as the corresponding PC or PB experiment but without the anomalous freshwater forcing over the North Atlantic. The errors caused by the model climate drift can be essentially eliminated by contrasting the twin experiments. Each experiment is integrated for 150 yr, and the last 100 yr are used for analyses. It should be noted that these experiments are used to assess not only the extratropical to tropical interaction over the Atlantic basin, but also the Atlantic-to-Pacific interbasin teleconnection, which will be discussed in the next section.

Without air–sea coupling over the extratropical North Atlantic in PC-xNA, the cooling is reduced substantially in the extratropics as surface air temperature is damped strongly toward the model SST climatology (Fig. 6). The cooling over the subtropical North Atlantic (10°–25°N) is also reduced significantly, to one-third of that in the FRESH-C experiment (Fig. 6a versus Fig. 3a) as the removal of extratropical SST-induced atmospheric teleconnection reduces the trade wind anomalies by half. The reduced anomalous advection in the ocean and atmosphere probably also contributes to the reduced response of tropical SST. In the deep tropics south of the equator (0°–10°S), the significant change is seen in winter and spring with the cold anomalies replaced in FRESH-C by weak warm anomalies, indicating an atmospheric teleconnection. The major warming in summer and fall is less affected, however (Fig. 6a).

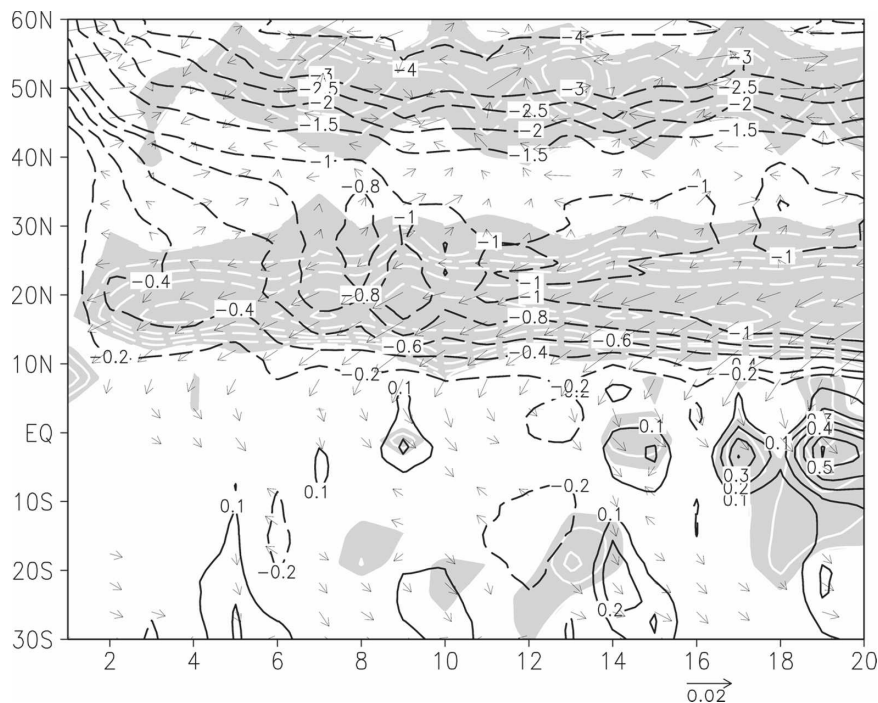


FIG. 7. Zonal mean SST ($^{\circ}\text{C}$), wind stress (vectors; N m^{-2}), and precipitation (shaded $>0.2 \text{ mm day}^{-1}$; contour interval at 0.1 mm day^{-1}) anomalies in the 10-member ensemble mean initial value experiments in response to 1-Sv watering that commences at $t = 0$ over the extratropical North Atlantic. All variables are averaged in time from June to December and zonally from 60°W to 20°E . Values (SST) over the shaded areas exceed the 95% statistical significance level using a t test.

The PC-xNA experiment demonstrates that the extratropical-tropical atmospheric teleconnection affects the tropical North Atlantic but may not be crucial for the development of SST anomalies on and south of the equator.

We now examine the effect of oceanic pathways in the extratropical-to-tropical teleconnection by shutting them off in the PB-NA experiment. In the PB-NA experiment, the imposed freshwater flux forcing leads to a similar coupled ocean-atmosphere response over the extratropical North Atlantic as that in the control simulation (Fig. 6b). The cooling over the tropical North Atlantic, however, is reduced substantially to only 20% of that in the FRESH-C experiment.¹ Most strikingly, the warming over the tropical South Atlantic virtually disappears (Fig. 6b). Thus the oceanic teleconnection plays a critical role in the development of the tropical Atlantic interhemispheric seesaw. This teleconnection

is presumably associated with coastal Kelvin wave and basin-scale Rossby wave adjustment (e.g., Cessi et al. 2004; Timmermann et al. 2005). In PB-NA, such wave adjustments to the AMOC shutdown are blocked from propagating into the tropics, and tropical changes in meridional ocean heat transport and thus oceanic temperature are much smaller than in FRESH-C (Fig. 5b).

b. Initial value problem

The role of oceanic teleconnection in the tropical Atlantic response can be further demonstrated in a spinup approach (Fig. 7). We carried 10-member ensemble experiments, each forced by the same freshwater flux over the North Atlantic and integrated for 20 yr with different initial conditions from the control simulation. Over the extratropical North Atlantic (north of 40°N), the cooling quickly reaches an equilibrium within 2–3 yr, associated predominantly with westerly wind anomalies. Over the subtropical North Atlantic (north of 15°N), the cooling also develops immediately and reaches an equilibrium in about a decade, suggesting a combination of fast atmospheric teleconnection and a slower oceanic adjustment. In the tropical Atlan-

¹ PB-NA probably underestimates atmospheric teleconnection effects as the entire water column in $30^{\circ}\text{--}40^{\circ}\text{N}$ is restored toward climatology, strongly damping SST variability in the latitudinal band.

tic (15°N–15°S), the cooling north of the equator almost immediately follows the extratropical North Atlantic and intensifies gradually. Associated with the cooling are northeasterly wind anomalies north of the equator and northerly cross-equatorial winds, which appear to quickly reach equilibrium. In contrast to the wind anomalies, the warming on and south of the equator, however, only emerges after about two decades, indicating the dominance of oceanic adjustments, consistent with the results of the PB-NA experiment. The precipitation anomalies in the tropical Atlantic appear to follow the development of South Atlantic SST anomalies, rather than the wind anomalies. The precipitation dipole emerges simultaneously with the development of the SST dipole (not shown), indicating the interaction between the ocean and atmosphere. Consistent with the PC-xNA and PB-NA experiments, results from the ensemble initial spinup experiments suggest a dominant role of oceanic adjustment in the deep tropical Atlantic response to the AMOC shutdown while the extratropical-to-tropical atmospheric teleconnection is a secondary contributing factor.

4. Atlantic-to-Pacific teleconnection

The effects of the AMOC shutdown extend far into the Pacific. This section discusses the Pacific response, first in the tropics and then the extratropics.

a. Tropical Pacific response

The annual mean response over the Pacific basin is characterized by a hemispheric seesaw pattern, with a substantial cooling in the midlatitudes, and a modest warming on and south of the equator (Fig. 2a). The maximum warming appears near the South America coast around 20°S, at 0.3°C in magnitude. The wind anomalies are characterized by an intensification of the westerlies in the midlatitudes and northerly cross-equatorial winds over the eastern equatorial Pacific (Fig. 2b). The warming in the equatorial Pacific results in a local increase in local rainfall at 1 mm (day K)⁻¹.

In general, the annual mean response over the tropical Pacific in our model appears to be weak but still in the range of other water-hosing experiments (Timmermann et al. 2007). The seasonal response is much stronger. Over the eastern tropical Pacific, weak cooling occupies the eastern equatorial Pacific in early spring (Fig. 8a), which appears to be associated with an intensification of the equatorial easterlies (Fig. 8b). This spring cooling is also evident in other coupled model simulations (e.g., Xie et al. 2007). In late spring, a dipolar SST anomaly develops (Fig. 8c), coupled with

anomalous northeasterly (northwesterly) winds north (south) of the equator (Fig. 8d). In the following summer and fall, the southern lobe (warm anomaly) of the dipole is amplified and extends both northward and westward (Fig. 8e). Associated with the westward extension, westerly wind anomalies develop along the equator, reducing equatorial upwelling and leading to a further development of the warm anomaly (Fig. 8f), much in line with the Bjerknes feedback. In the following winter, substantial warming anomalies appear over the entire equatorial region (Figs. 8g,h), resembling the model-simulated El Niño (Liu et al. 2000). The maximum warming is located in the central Pacific, with a magnitude of 0.7°C.

The seasonal response of the tropical Pacific to the shutdown of the AMOC is consistent with a previous study using the same GCM. In Wu et al. (2005), a cold SST anomaly over the tropical North Atlantic (TNA) induces a SST dipole in the eastern tropical Pacific, with the cold and warm anomaly north and south of the equator, respectively. The cold NTA anomaly suppresses convection and rainfall over the Caribbean Basin, producing a surface high extending to the eastern tropical North Pacific. This atmospheric response appears to be most pronounced in late spring and summer with strong convection over the Caribbean Basin (Wang and Enfield 2001). Over the eastern tropical Pacific, this anomalous high induces northeasterly wind anomalies north, northerly cross-equatorial winds, and northwesterly winds (due to Coriolis force) south of the equator (Fig. 8d). This C-shape wind anomaly generates a dipolar SST anomaly through changes in surface evaporation (Fig. 8c). This coupled WES feedback, which has been extensively studied in relation to tropical Atlantic variability (see a recent review by Xie and Carton 2004), acts to amplify the SST dipole. During boreal summer, the mean cross-equatorial winds are southerly, inducing intense upwelling slightly south of the equator that is key to the development of the mean cold tongue (Philander and Pacanowski 1981; de Szoek et al. 2007). In the water-hosing experiment, the northerly anomalies associated with the SST dipole cause an equatorial warming by reducing the southern upwelling. The resultant warming on the equator develops into an El Niño-like pattern, amplified by the Bjerknes feedback (Fig. 8g).

The seasonal development of the equatorial Pacific response is further summarized in time–longitude plots of SST, zonal wind, and upper-100-m heat content (Fig. 9). The equatorial warming initiates in late spring shortly after northwesterly anomalies appear in the Far East. The warming propagates subsequently toward the west, reaching a maximum of 0.8°C in December

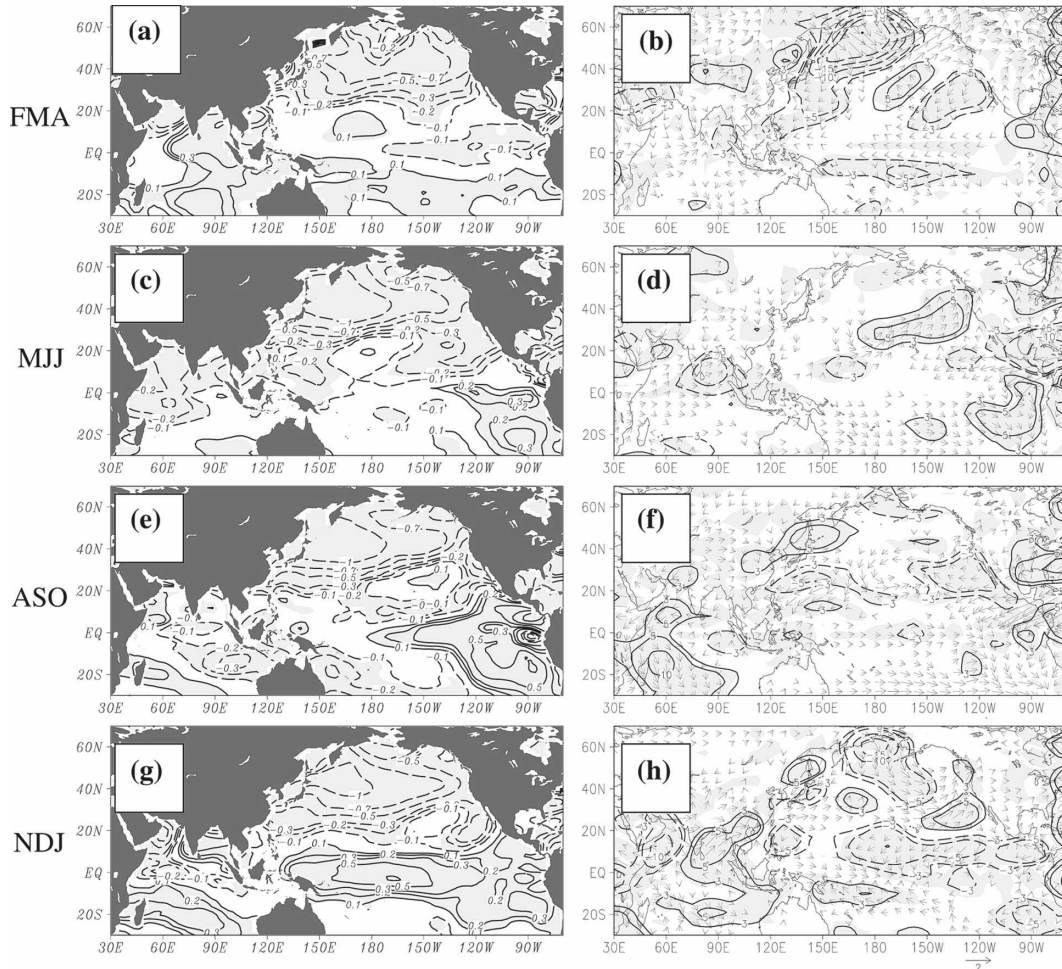


FIG. 8. Seasonally stratified anomalies in FRESH-C. (left) SST ($^{\circ}\text{C}$); (right) surface wind stress (vectors; N m^{-2}) and turbulent heat flux (W m^{-2} ; positive-downward). Plotted values are significant at the 95% statistical significance level using a t test.

around the date line (Fig. 9a). The westward propagation is due to the phase shift between anomalies of SST and zonal wind (Neelin 1991): the SST warming induces westerly wind anomalies to the west, which reduce the equatorial upwelling and move the warming westward. The same mechanism operates to generate the westward propagation of the equatorial annual cycle in SST over the equatorial Pacific (Xie 1994). In response to the westerly wind anomalies in FRESH-C, the subsurface also starts to warm from summer, with the maximum located in the eastern equatorial Pacific, indicating a relaxation of the equatorial thermocline tilt (Fig. 9b) that reinforces the surface warming via the thermocline feedback. We note that there are some cold SST anomalies, albeit weak, starting in February in the eastern equatorial Pacific with a subsequent westward propagation. The cooling in the subsurface becomes pronounced from late winter to early summer in the

eastern equatorial Pacific, indicating a shoaling of the equatorial thermocline during this period. Thus, the equatorial annual cycle in SST weakens in the water-hosing experiment, but changes in the annual mean thermocline are negligible.

The previous diagnosis suggests the importance of the tropical North Atlantic in inducing the tropical Pacific response. To demonstrate this role explicitly, we conduct a sensitivity experiment in which the air-sea coupling over the tropical Atlantic (20°S – 25°N) is disabled (PC-TA). In PC-TA, equatorial SST anomalies are much reduced. In particular, there is no El Niño-like SST warming over the tropical Pacific (Fig. 9c). Thus the tropical Atlantic is an important conduit for the AMOC influence on the tropical Pacific, in line with an earlier idealized model studies (Wu et al. 2005). This experiment also indicates that the tropical atmospheric teleconnection is much more effective

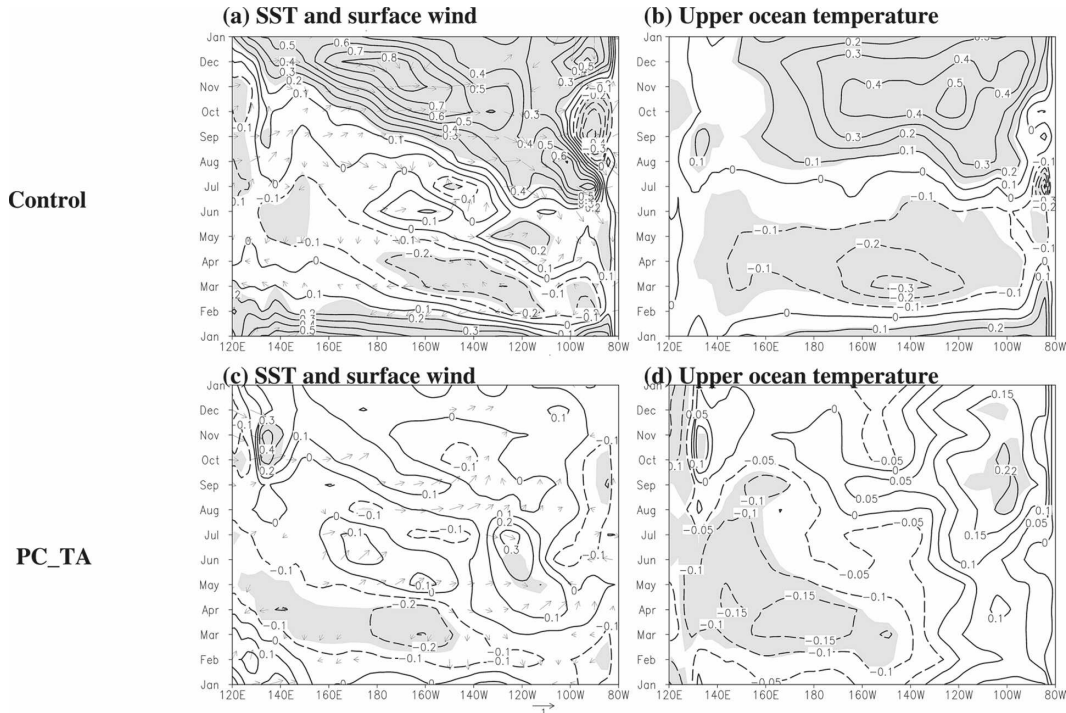


FIG. 9. Time-longitude plots of (left) equatorial Pacific SST (contours) and surface wind (vectors; m s^{-1}) and (right) upper-150-m-averaged temperature anomalies (unit: $^{\circ}\text{C}$) for (a), (b) CTRL and (c), (d) PC-TA. All variables are averaged over (5°S , 5°N). Values (temperature) over the shaded areas exceed the 95% statistical significance level using a t test.

than the oceanic one in inducing tropical Pacific anomalies.

We note, however, that the boreal spring cooling, while weak, remains in the western and central equatorial Pacific (Figs. 9c,d). The following two subsections present evidence that this weak cooling is due to the extratropical-to-tropical interaction within the Pacific triggered by the atmospheric teleconnection from the extratropical North Atlantic.

b. North Pacific response

The cooling over the midlatitude North Pacific is another prominent feature in our water-hosing experiment, as is in other GCMs (Timmermann et al. 2007). The maximum cooling is about 1°C located in the midlatitude western Pacific (Fig. 2a). The cooling over the western North Pacific also exhibits a seasonal dependence with the maximum and the minimum respectively in late summer and winter (Fig. 10a).

The extratropical Atlantic-to-Pacific atmospheric teleconnection provides an important forcing in generating the cooling over the North Pacific. Over the western and central North Pacific, the cooling is associated with an intensification of both latent and sensible heat

loss during much of the year (Figs. 11a,b,e). In summer, the cooling appears to be associated with a reduction of shortwave radiation flux due to an increase of marine stratus clouds (Figs. 11d,e). In the western North Pacific, the cooling is further intensified by anomalous cold advection (Fig. 11f). This cold advection persists year round and is largely due to the anomalous southward flow forced by the interior cyclonic wind stress anomalies (Fig. 2a). The effects of the surface Ekman flow are not important because no persistent westerly anomalies appear in this region during much of the year. This is in contrast to the eastern North Pacific where the surface Ekman cold advection plays a dominant role except in summer (Figs. 11e,f). We have examined the vertical structure of current anomalies, and indeed, the anomalous southward flow trapped in the top 40m dominates in the eastern half of the basin (not shown).

The heat budget analysis indicates that the strengthening of the midlatitude westerly and the Aleutian low associated with the AO-like dynamic response forced by the extratropical North Atlantic cooling plays an important role in forcing the cooling in the North Pacific through both the changes of the surface heat flux and the oceanic advection. The intensification of the

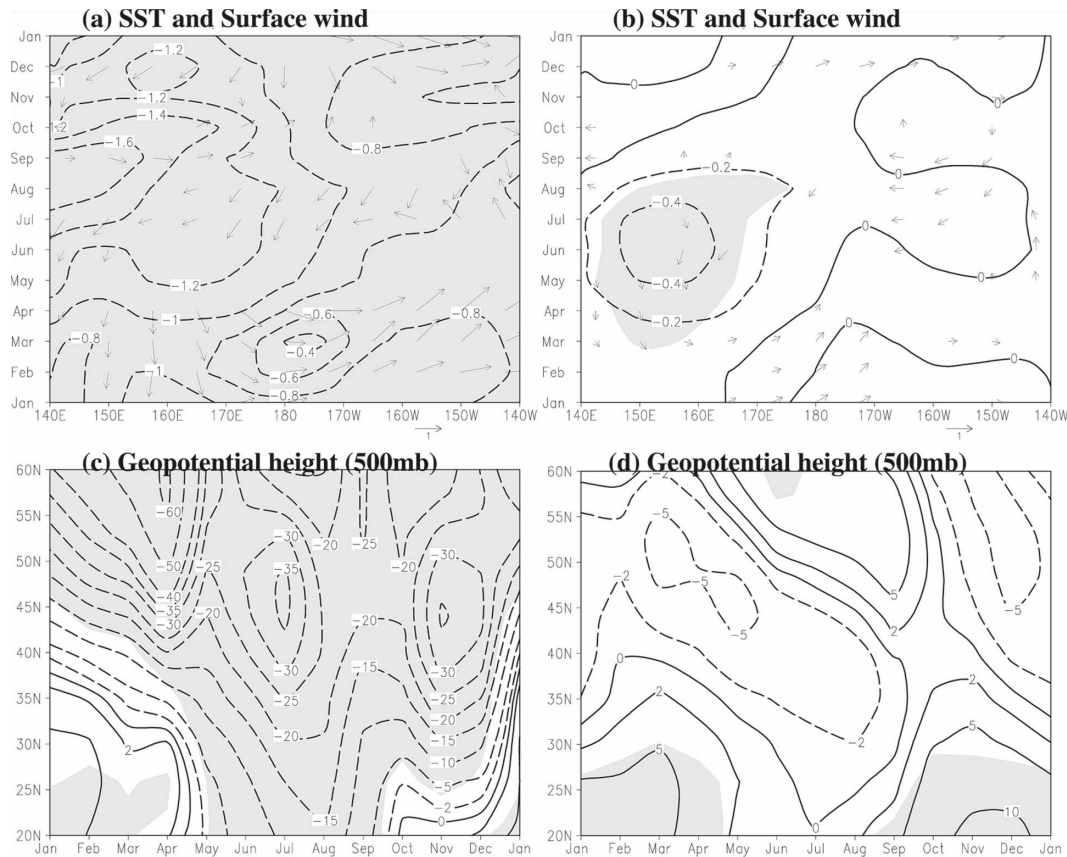


FIG. 10. Time–longitude plots of SST and surface wind velocity (m s^{-1}) anomalies averaged within the latitudinal band (35° – 45° N), and time–latitude plots of geopotential height on 500-mb level averaged within (170° E, 160° W) for (a), (c) FRESH-C and (b), (d) PC-xNA. Values (upper panel for SST only) over the shaded areas exceed the 95% statistical significance level using a t test.

sensible heat loss during winter and early spring, however, may also reflect the mean advection from the North Atlantic to the North Pacific by the mean westerly.

Over the North Pacific, the atmospheric response tends to be dominated by equivalent barotropic low in all seasons although its center of action shifts in time (Fig. 10c). This circumglobal teleconnection is a reminiscent of the Arctic Oscillation, the leading mode of Northern Hemispheric atmosphere variability in winter (Thompson and Wallace 1998). The extratropical circulation anomalies are due largely to the atmospheric response to extratropical SST anomalies. In the PC-TA experiment where the air–sea coupling over the tropical Atlantic and thus the El Niño–like anomalies in the tropical Pacific are eliminated, the extratropical North Pacific atmospheric response remains similar to that in the fully coupled model (not shown). In contrast, The PC-xNA experiment, in which the air–sea coupling over the extratropical North Atlantic is disabled, the

atmospheric low and midlatitude cooling over the North Pacific are virtually eliminated (Figs. 10b,d). The extratropical atmospheric teleconnection that transmits the effects of the North Atlantic cooling to the midlatitude North Pacific may involve the AO-like circumglobal mode and/or the advection by the mean westerly wind jet.

c. Extratropical-to-tropical influence in the Pacific basin

The North Pacific can be an additional conduit of the AMOC influence on the tropical Pacific as alluded to in section 4a. The PC-TA experiment illustrates this process, in which atmospheric teleconnection from the tropical Atlantic is eliminated. A southwestward propagation of SST from the coast of Baja California toward the equator is seen from early winter to spring (Fig. 12). This propagation is coupled with an intensification of the northeasterly trade winds on the south edge of the

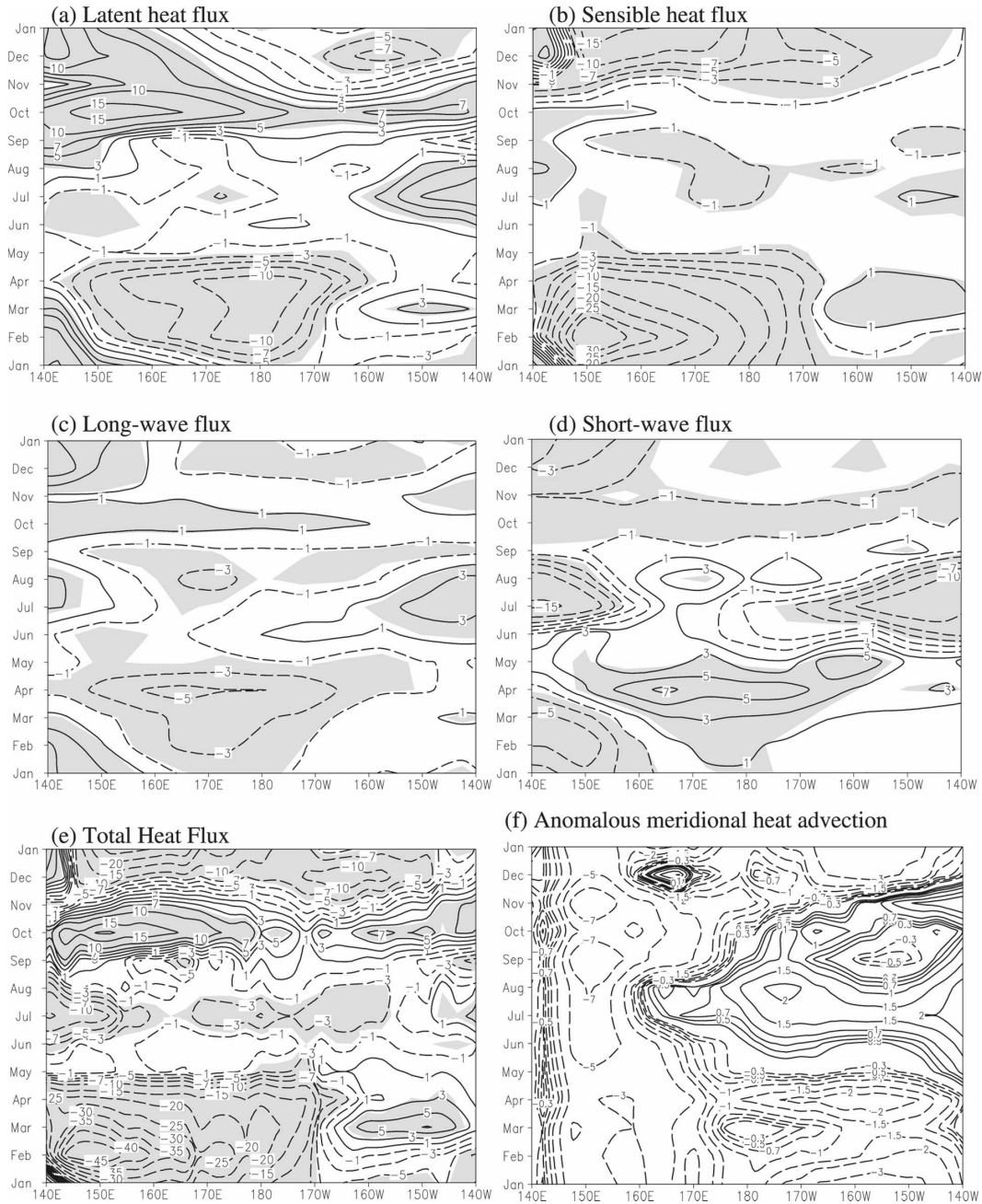


FIG. 11. Time-longitude plots of (a) latent, (b) sensible, (c) longwave, (d) shortwave, and (e) total heat flux (downward-positive), and (f) oceanic anomalous meridional heat transport (integrated over upper 100 m). All quantities are averaged within latitudinal band (40°–50°N). Units are $W m^{-2}$.

SST cooling, an interaction that may be interpreted in a broad sense as WES feedback. A cold SST anomaly in the eastern subtropical Pacific induces an anomalous high in pressure, which generates easterly wind anomalies on the equatorward flank. These easterly wind anomalies accelerate the mean northeast trade winds, enhancing oceanic evaporative heat loss to induce cooling on the equatorward flank of the original SST cool-

ing and causing the coupled SST–wind pattern to propagate equatorward. This coupled interaction between the atmospheric boundary layer and SST has been invoked to explain the equatorial Pacific annual cycle (Liu and Xie 1994) and tropical Pacific decadal climate variability (Wu et al. 2007b). It is also similar to the finger printing mechanism of Vimont et al. (2003).

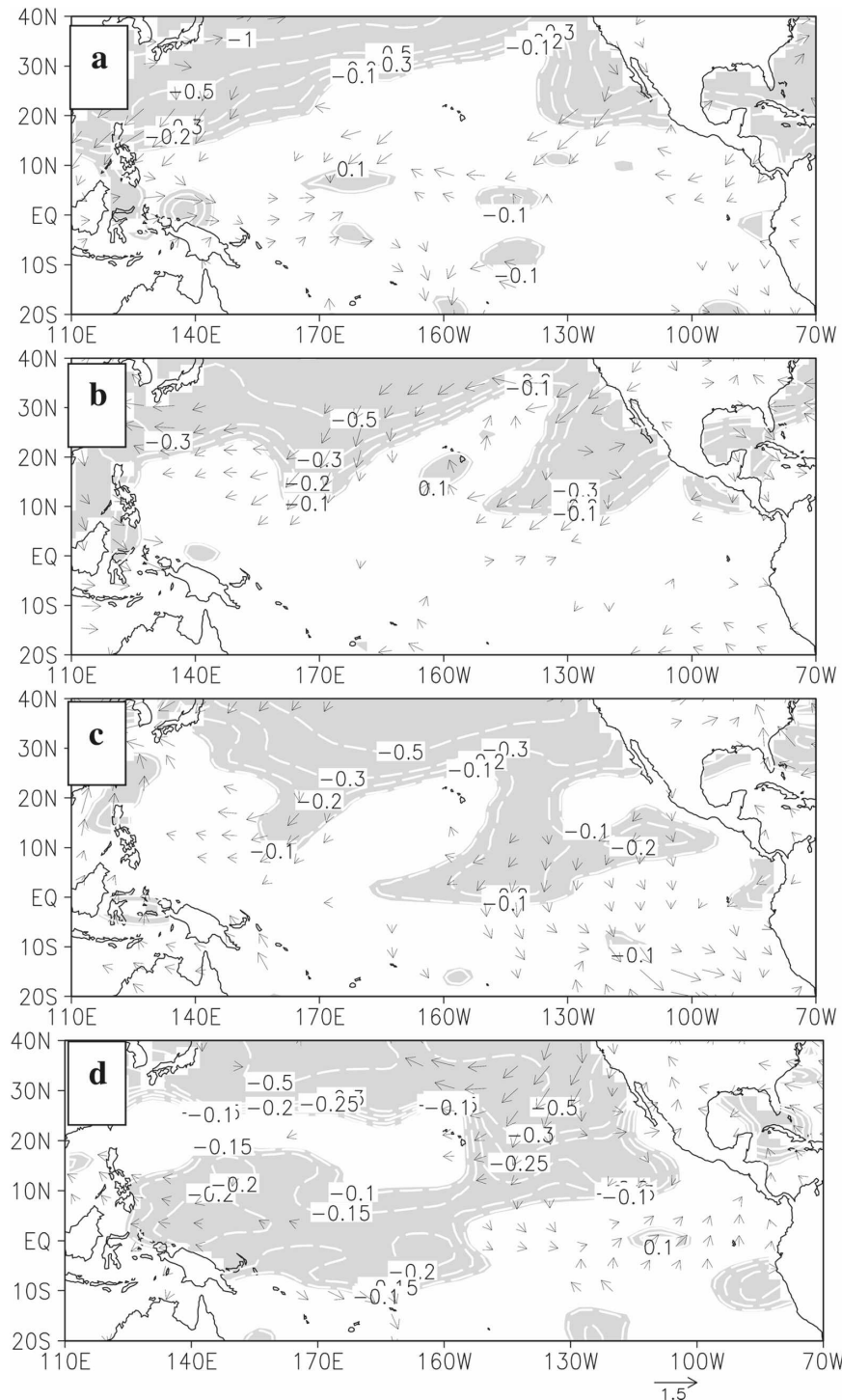


FIG. 12. Pacific SST ($^{\circ}\text{C}$) and surface wind (vectors; m s^{-1}) anomalies in PC-TA for (a) October, (b) December, (c) February, and (d) April. Shaded SST anomalies and wind plotted are significant at the 95% statistical significance level using a t test.

This subtropical WES pathway is active in the boreal spring, and it produces SST anomalies over the western and central equatorial Pacific of the same sign as those in the North Atlantic. In contrast, the tropical telecon-

nection from the tropical Atlantic is active in late spring and summer, and it generates ENSO-like SST anomalies with an opposite polarity to those in the North Atlantic. In terms of relative importance, the latter

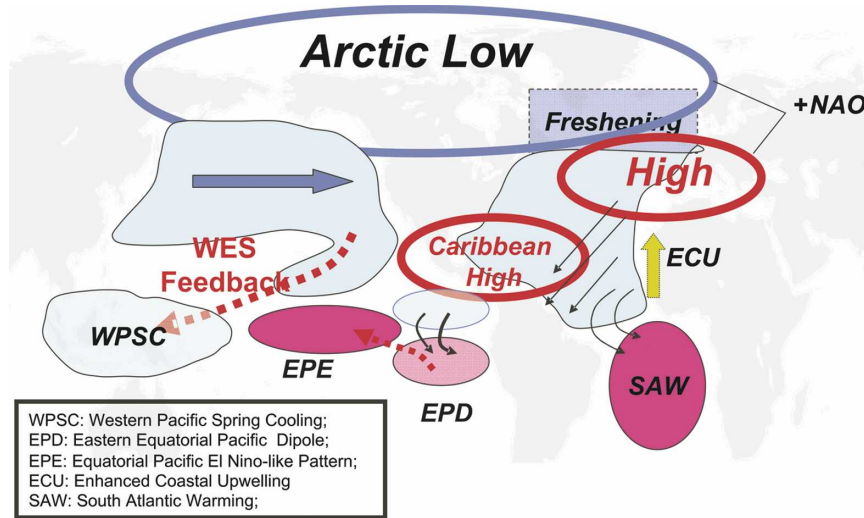


FIG. 13. Schematic diagram of global teleconnections in response to AMOC shutdown.

tropical teleconnection generates larger tropical Pacific anomalies than the subtropical WES pathway.

5. Summary and discussions

We have conducted a water-hosing simulation to study the global teleconnections in response to a shutdown of the AMOC. A series of sensitivity experiments shed further light on key ocean–atmospheric processes involved in the teleconnections. Major findings are summarized in a schematic diagram in Fig. 13 and in the text as follows:

- 1) The large freshwater flux over the subpolar North Atlantic immediately shuts off the deep convection, causes an intense local cooling, and hauls the AMOC to a stop within 2–3 decades.
- 2) The cooling over the extratropical North Atlantic forces an AO–NAO-like response, intensifying the midlatitude westerlies and the northeast trades. The latter change in the trades helps generate cold SST anomalies by increasing oceanic turbulent heat loss and vertical upwelling over the western and eastern subtropical North Atlantic, respectively.
- 3) SST increases on and south of the equator in the tropical Atlantic through anomalous meridional and vertical advection. This tropical SST dipole, coupled with the C-shape wind anomalies, is most pronounced in boreal summer and fall, causing a southward shift of the Atlantic ITCZ.
- 4) The cooling over the tropical North Atlantic forces an anomalous Caribbean high, intensifying northeast trades across Central America and triggering a meridional dipole over the eastern Pacific by the WES feedback in boreal spring, with negative and

positive SST anomalies north and south of the equator, respectively. The associated atmospheric adjustment reduces the southerly cross-equatorial wind and ocean upwelling, inducing an equatorial warming that develops into an El Niño–like pattern in fall by the Bjerknes feedback.

- 5) Over the extratropical North Pacific, the Aleutian low deepens and the midlatitude westerlies intensify, causing a basinwide cooling. The cooling is also likely intensified by the mean westerly advection.
- 6) The North Pacific cooling off Baja California propagates southwestward in spring through the coupled WES feedback, reaching in the western equatorial Pacific.

Our sensitivity experiments provide a useful modeling framework to decipher the dynamic processes in transmitting the influences of the AMOC around the global. The PB-NA experiment demonstrates that oceanic adjustments play a dominant role in the formation of the tropical SST dipole that displaces the ITCZ southward. The PC-TA experiment illustrates the critical role of tropical Atlantic air–sea coupling in generating the El Niño–like response over the equatorial Pacific through the tropical atmospheric teleconnection. The PC-xNA experiment shows that the atmospheric teleconnection induced by the extratropical North Atlantic cooling is key to the basinwide cooling over the midlatitude North Pacific through the annular mode as well as the advection by the mean westerlies. Krebs and Timmermann (2007) conducted similar sensitivity experiments and showed that tropical Atlantic ocean–atmosphere interaction accelerates the recovery of the AMOC after the cessation of water hosing.

The present study offers a physical basis for interpreting the coherence of various paleoclimate observations around the globe with the Dansgaard–Oeschger cycles, which are often associated with Heinrich events of massive land ice sheet discharges into the North Atlantic. Indeed, there is paleo-observational evidence for coherent covariability in subpolar North Pacific SST with the Greenland ice core record (Harada et al. 2006), consistent with this and other water-hosing experiments. In the instrumental record, SST variability is much more modest but observations suggest in-phase SST variability between the North Atlantic and the North Pacific in the so-called Atlantic multidecadal oscillation (e.g., Enfield et al. 2001). Some modeling studies also report a Northern Hemispheric resonance mode with the North Atlantic and Pacific varying in sync (e.g., Timmermann et al. 1998; Wu and Liu 2005). Much needs to be learned about AMOC-induced climate variability and the role of air–sea interaction in shaping its space–time patterns.

Acknowledgments. This work is supported by the Zhufeng and Green Card Projects of the Ocean University of China with funding provided by the Chinese Ministry of Education, National Science Foundation of China (NSFC) Outstanding Youth Program (40788002), and NSFC Grants (40756009 and 90411010). SPX is supported by the NOAA CLIVAR Program, and the Japan Agency for Ocean–Earth Science and Technology. We are indebted to both reviewers for their constructive comments, which greatly improved the paper in many aspects. All calculations were performed in the Supercomputing Center of Ocean University of China. Discussions with Drs. Jiayan Yang and Fritz Schott were helpful.

REFERENCES

- Barnett, T. P., D. W. Pierce, M. Latif, D. Dommenges, and R. Saravanan, 1999: Interdecadal interactions between the tropics and midlatitudes in the Pacific basin. *Geophys. Res. Lett.*, **26**, 615–618.
- Black, D. E., L. C. Peterson, J. T. Overpack, A. Kaplan, M. N. Evans, and M. K. Kshgarian, 1999: Eight centuries of North Atlantic ocean atmosphere variability. *Science*, **286**, 1709–1713.
- Broecker, W. S., 1991: The great ocean conveyor. *Oceanography*, **4**, 79–89.
- , 2003: Does the trigger for abrupt climate change reside in ocean or in the atmosphere? *Science*, **300**, 1519–1522.
- Cessi, P., K. Bryan, and R. Zhang, 2004: Global seiching of thermocline waters between the Atlantic and the Indian-Pacific Ocean basins. *Geophys. Res. Lett.*, **31**, L04302, doi:10.1029/2003GL019091.
- Chiang, J. C. H., 2004: Present-day climate variability in the tropical Atlantic: A model for paleoclimate changes? *The Hadley Circulation: Past, Present, and Future*, H. F. Diaz and R. Bradley, Eds., Springer, 465–488.
- , and A. Koutavas, 2004: Tropical flip-flop connections. *Nature*, **432**, 684–685.
- Curry, R., B. Dickson, and I. Yashayaev, 2003: A change in the freshwater balance of the Atlantic Ocean over the past four decades. *Nature*, **426**, 826–829.
- Czaja, A., P. van der Vaart, and J. Marshall, 2002: A diagnostic study of the role of remote forcing in tropical Atlantic variability. *J. Climate*, **15**, 3280–3290.
- de Szoeke, S. P., S.-P. Xie, T. Miyama, K. J. Richards, and R. J. O. Small, 2007: What maintains the SST front north of the eastern Pacific equatorial cold tongue? *J. Climate*, **20**, 2500–2514.
- Dong, B.-W., and R. T. Sutton, 2002: Adjustment of the coupled ocean–atmosphere system to a sudden change in the thermohaline circulation. *Geophys. Res. Lett.*, **29**, 1728, doi:10.1029/2002GL015229.
- , and —, 2007: Enhancement of ENSO variability by a weakened Atlantic thermohaline circulation in a coupled GCM. *J. Climate*, **20**, 4920–4939.
- Enfield, D. B., A. M. Mestas-Nunez, and P. J. Trimble, 2001: The Atlantic multidecadal oscillation and its relation to rainfall and river flows in the continental U.S. *Geophys. Res. Lett.*, **28**, 2077–2080.
- Goodman, P. J., 2001: Thermohaline adjustment and advection in an OGCM. *J. Phys. Oceanogr.*, **31**, 1477–1497.
- Harada, N., N. Ahagon, T. Sakamoto, M. Uchida, M. Ikehara, and Y. Shibata, 2006: Rapid fluctuation of alkenone temperature in the southwestern Okhotsk Sea during the past 120 ky. *Global Planet. Change*, **53**, 29–46.
- Hemming, S. R., 2004: Heinrich events: Massive late Pleistocene detritus layers of the North Atlantic and their global climate imprint. *Rev. Geophys.*, **42**, RG1005, doi:10.1029/2003RG000128.
- Hoskins, B. J., and D. J. Karoly, 1981: The steady linear response of a spherical atmosphere to thermal and orographic forcing. *J. Atmos. Sci.*, **38**, 1179–1196.
- Jacob, R. L., 1997: Low frequency variability in a simulated atmosphere ocean system. Ph.D. thesis, University of Wisconsin—Madison, 155 pp.
- Krebs, U., and A. Timmermann, 2007: Tropical air–sea interactions accelerate the recovery of the Atlantic Meridional Overturning Circulation after a major shutdown. *J. Climate*, **20**, 4940–4956.
- Kushnir, Y., W. A. Robinson, I. Blade, N. M. J. Hall, S. Peng, and R. Sutton, 2002: Atmospheric GCM response to extratropical SST anomalies: Synthesis and evaluation. *J. Climate*, **15**, 2233–2256.
- Liu, Z., and S.-P. Xie, 1994: Equatorward propagation of coupled air–sea disturbances with application to the annual cycle of eastern tropical Pacific. *J. Atmos. Sci.*, **51**, 3807–3822.
- , and M. A. Alexander, 2006: Atmospheric bridge, oceanic tunnel, and global climatic teleconnections. *Rev. Geophys.*, **45**, RG2005, doi:10.1029/2005RG000172.
- , J. Kutzbach, and L. Wu, 2000: Modeling climatic shift of El Niño in the Holocene. *Geophys. Res. Lett.*, **27**, 2265–2268.
- Manabe, S., and R. Stouffer, 1988: Two stable equilibria of a coupled ocean–atmosphere model. *J. Climate*, **1**, 841–866.
- , and —, 1995: Simulation of abrupt climate change induced by freshwater input to the North Atlantic Ocean. *Nature*, **378**, 165–167.
- Marshall, J., and Coauthors, 2001: North Atlantic climate vari-

- ability: Phenomena, impacts and mechanisms. *Int. J. Climatol.*, **21**, 1863–1898.
- McCreary, J. P., and P. Lu, 1994: Interaction between the subtropical and equatorial ocean circulation: The subtropical cell. *J. Phys. Oceanogr.*, **24**, 466–497.
- Neelin, J. D., 1991: The slow sea surface temperature mode and the fast-wave limit: Analytic theory for tropical interannual oscillations and experiments in a hybrid coupled model. *J. Atmos. Sci.*, **48**, 584–606.
- Okajima, H., S.-P. Xie, and A. Numaguti, 2003: Interhemispheric coherence of tropical climate variability: Effect of climatological ITCZ. *J. Meteor. Soc. Japan*, **81**, 1371–1386.
- Okumura, Y., S.-P. Xie, A. Numaguti, and Y. Tanimoto, 2001: Tropical Atlantic air-sea interaction and its influence on the NAO. *Geophys. Res. Lett.*, **28**, 1507–1510.
- Pahnke, K., J. P. Sachs, L. Keigwin, A. Timmermann, and S.-P. Xie, 2007: Eastern tropical Pacific hydrologic changes during the past 27,000 years from D/H ratios in alkenones. *Paleoceanography*, **22**, PA4214, doi:10.1029/2007PA001468.
- Peng, S., W. A. Robinson, and S. Li, 2003: Mechanisms for the NAO responses to the North Atlantic SST tripole. *J. Climate*, **16**, 1987–2004.
- Peterson, L. C., G. H. Haug, K. A. Hughen, and U. Rohl, 2000: Rapid changes in the hydrological cycle of the tropical Atlantic during the last glacial. *Science*, **290**, 1947–1951.
- Philander, S. G. H., and R. C. Pacanowski, 1981: The oceanic response to cross-equatorial winds (with application to coastal upwelling in low latitudes). *Tellus*, **33**, 201–210.
- Stouffer, R., and Coauthors, 2006: Investigating the causes of the response of the thermohaline circulation to past and future climate changes. *J. Climate*, **19**, 1365–1387.
- Talley, L., J. Reid, and P. Robbins, 2003: Date-based meridional overturning streamfunction for the global ocean. *J. Climate*, **16**, 3213–3226.
- Thompson, D. W. J., and J. M. Wallace, 1998: The Arctic Oscillation signature in the wintertime geopotential height and temperature fields. *Geophys. Res. Lett.*, **25**, 1297–1300.
- Timmermann, A., M. Latif, R. Voss, and A. Grötzner, 1998: Northern Hemispheric interdecadal variability: A coupled air-sea mode. *J. Climate*, **11**, 1906–1931.
- , S. An, U. Krebs, and H. Goosse, 2005: ENSO suppression due to a weakening of the North Atlantic thermohaline circulation. *J. Climate*, **18**, 3122–3139.
- , and Coauthors, 2007: The influence of a weakening of the Atlantic meridional overturning circulation on ENSO. *J. Climate*, **20**, 4899–4919.
- Vellinga, M., R. Wood, and J. M. Gregory, 2002: Processes governing the recovery of a perturbed thermohaline circulation in HadCM3. *J. Climate*, **15**, 764–779.
- Vimont, D. J., J. M. Wallace, and D. S. Battisti, 2003: The seasonal footprinting mechanism in the Pacific: Implications for ENSO. *J. Climate*, **16**, 2668–2675.
- Wang, C., and D. B. Enfield, 2001: The tropical western hemisphere warm pool. *Geophys. Res. Lett.*, **28**, 1635–1638.
- Wang, X., A. S. Auler, R. L. Edwards, H. Cheng, P. S. Cristalli, P. L. Smart, D. A. Richards, and C. C. Shen, 2004: Wet periods in northeastern Brazil over the past 210 kyr linked to distant climate anomalies. *Nature*, **432**, 740–743.
- Weaver, A. J., C. M. Bitz, A. F. Faming, and M. M. Holland, 1999: Thermohaline circulation: High-latitude phenomena and the difference between the Pacific and Atlantic. *Annu. Rev. Earth Planet. Sci.*, **27**, 231–285.
- Wu, L., and Z. Liu, 2002: Is tropical Atlantic variability driven by the North Atlantic Oscillation? *Geophys. Res. Lett.*, **29**, 1653, doi:10.1029/2002GL014939.
- , and —, 2005: North Atlantic decadal variability: Air-sea coupling, oceanic memory, and potential northern hemisphere resonance. *J. Climate*, **18**, 331–349.
- , —, R. Gallimore, R. Jacob, Y. Zhong, and D. Lee, 2003: Pacific decadal variability: The Tropical Pacific Mode and the North Pacific Mode. *J. Climate*, **16**, 1101–1120.
- , F. He, and Z. Liu, 2005: Coupled ocean-atmosphere response to north tropical Atlantic SST: Tropical Atlantic dipole and ENSO. *Geophys. Res. Lett.*, **32**, L24710, doi:10.1029/2005GL024812.
- , —, —, and C. Li, 2007a: Atmospheric teleconnection of tropical Atlantic variability: Interhemispheric, tropical-extratropical, and cross-basin interaction. *J. Climate*, **20**, 856–870.
- , Z. Liu, C. Li, and Y. Sun, 2007b: Extratropical control of recent tropical decadal climate variability: A relay teleconnection. *Climate Dyn.*, **28**, 99–112.
- Xie, S.-P., 1994: On the genesis of the equatorial annual cycle. *J. Climate*, **7**, 2008–2013.
- , and S. G. H. Philander, 1994: A coupled ocean-atmosphere model of relevance to the ITCZ in the eastern Pacific. *Tellus*, **46A**, 340–350.
- , and Y. Tanimoto, 1998: A pan-Atlantic decadal climate oscillation. *Geophys. Res. Lett.*, **25**, 2185–2188.
- , and J. A. Carton, 2004: Tropical Atlantic variability: Patterns, mechanism, and impacts. *Earth Climate: The Ocean-Atmosphere Interaction*, *Geophys. Monogr.*, Vol. 147, Amer. Geophys. Union, 121–142.
- , and Coauthors, 2007: A regional ocean-atmosphere model for eastern Pacific climate: Toward reducing tropical biases. *J. Climate*, **20**, 1504–1522.
- Yang, J., 1999: A linkage between decadal climate variations in the Labrador Sea and the tropical Atlantic Ocean. *Geophys. Res. Lett.*, **26**, 1023–1026.
- Zhang, R., and T. Delworth, 2005: Simulated tropical response to a substantial weakening of the Atlantic thermohaline circulation. *J. Climate*, **18**, 1853–1860.